Available online at www.sciencedirect.com
SCIENCE DIRECT®
Journal of Organometallic Chemistry 689 (2004) 4897–4908
Journal of Organometallic Chemistry
www.elsevier.com/locate/jorganchem

Organosilicon hypersilylchalcogenolates and related compounds

Heike Lange [a], Uwe Herzog [a,*], Horst Borrmann [b], Bernhard Walfort [c]

[a] Institut für Anorganische Chemie, TU Bergakademie Freiberg, Leipziger Straße 29, D-09596 Freiberg, Germany
[b] Max-Planck-Institut für Chemische Physik fester Stoffe, Nöthnitzer Straße 40, D-01187 Dresden, Germany
[c] Institut für Chemie, TU Chemnitz, Straße der Nationen 62, D-09111 Chemnitz, Germany

Received 24 February 2004; accepted 28 June 2004
Available online 2 November 2004

Abstract

Reaction of potassium hypersilylchalcogenolates $(Me_3Si)_3SiEK$ (E = S, Se, Te) with organochlorosilanes $R_{4-x}SiCl_x$ (R = Me, Ph; x = 1–4) and methylchlorodisilanes (Si_2Me_5Cl, 1,2-$Si_2Me_4Cl_2$) yields organosilicon hypersilylchalcogenolates $[(Me_3Si)_3SiE]_xSiR_{4-x}$ (x = 1–4) and $[(Me_3Si)_3SiE]_xSi_2Me_{6-x}$ (x = 1, 2). A partial substitution product, $[(Me_3Si)_3SiSe]_2SiPhCl$ (**2**) has been obtained by reaction of $PhSiCl_3$ with 1.5 equivalents $(Me_3Si)_3SiSeK$. Besides characterization by ^{1}H, ^{13}C, ^{29}Si, ^{77}Se and ^{125}Te NMR spectroscopy the compounds $[(Me_3Si)_3SiTe]_2SiPh_2$ (**1**), $[(Me_3Si)_3SiSe]_2SiPhCl$ (**2**) and $[(Me_3Si)_3SiSe]_2Si_2Me_4$(**3**) have also been analyzed by crystal structure analyses.

Starting from $(Me_3Si)_5Si_2K$ treatment with sulfur gave the highly branched potassium heptasilanylthiolate $(Me_3Si)_5Si_2SK$. Reactions with methylchlorosilanes $Me_{4-x}SiCl_x$ (x = 1, 2, 3) yielded organosilicon heptasilanylthiolates $[(Me_3Si)_3Si–(Me_3Si)_2Si–S]_xSiMe_{3-x}$.

Keywords: Hypersilyl; Chalcogene; Silicon

1. Introduction

Besides simple disilylchalcogenides $R_3Si–E–SiR_3$ (E = S, Se, Te) the chemistry of organosilicon chalcogen compounds is dominated by cyclic and polycyclic structures. Some of the most important types of ring systems are shown in Scheme 1 [1–25].

As can be seen from Scheme 1 all structures are built of four-, five- and six-membered rings. The strong tendency to from cyclic products as well as the preferential formation of rather small rings results from the small bond angles Si–E–Si in contrast to increased bond angles at oxygen in siloxanes. The small bond angles at sulfur, selenium or tellurium reflect the high p character of the bond orbitals at the heavier chalcogen atoms.

Aim of this work is the formation of acyclic organosilicon chalcogen compounds $R_{4-x}Si[–E–SiR'_3]_x$ (E = S, Se, Te). To prevent the formation of cyclic or polycyclic products the bulky hypersilyl unit as well as even larger highly branched organooligosilanyl units were employed.

Arnold et al. have shown that starting from hypersilyltellurol, $(Me_3Si)_3SiTeH$, reactions with a variety of main group elements as well as transition metal derivatives (e.g. halogenides, bis(trimethylsilyl)amides) lead to hypersilyltellurolates of these elements [26–33]. Hypersilyltellurol has been obtained by insertion of elemental tellurium into the Si–Li bond of hypersilyllithium [34] (prepared by cleavage of $Si(SiMe_3)_4$ with MeLi [35]) and subsequent reaction with HCl [36] or triflic acid [37,38].

* Corresponding author. Tel.: +49 3731 394343; fax: +49 3731 394058.
E-mail address: uwe.herzog@chemie.tu-freiberg.de (U. Herzog).

0022-328X/$ - see front matter © 2004 Elsevier B.V. All rights reserved.
doi:10.1016/j.jorganchem.2004.06.067

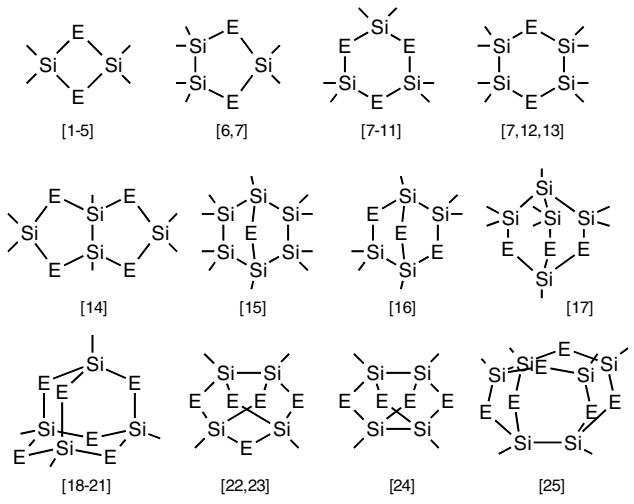

Scheme 1. Selection of most important types of ring systems in organosilicon chalcogenides (E = S, Se, Te) [1–25].

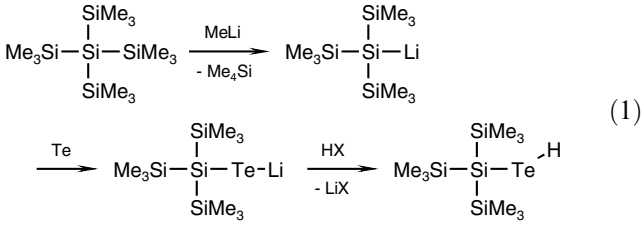

(1)

Lithium hypersilylselenolate and -thiolate have been obtained by chalcogen metathesis reactions starting from hypersilyltellurolate [39]:

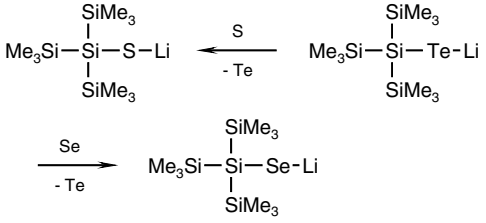

(2)

More recently, the reaction of $Si(SiMe_3)_4$ with KO^tBu developed by Marschner [40], has made $KSi(SiMe_3)_3$ and a variety of other oligosilanylpotassium species [41–43] readily available. As we have shown in a previous report [44], treatment of $KSi(SiMe_3)_3$ with elemental chalcogen (sulfur, selenium, tellurium) in THF yields the corresponding potassium hypersilylchalcogenolates $K[ESi(SiMe_3)_3]$:

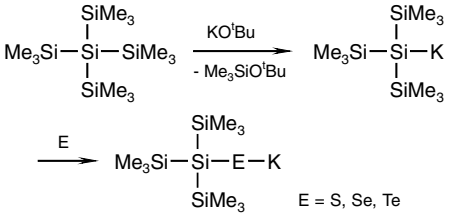

2. Results and discussion

2.1. Organosilicon hypersilylchalcogenolates

Starting from organochlorosilanes $R_{4-x}SiCl_x$ (R = Me, Ph; x = 1–4) reactions with potassium hypersilylchalcogenolates yield organosilicon hypersilylchalcogenolates as shown in Scheme 2.

In some cases, especially in reactions with $MeSiCl_3$, a side reaction resulting from a chalcogen halogen exchange has been observed. This reaction led to hypersilyl chloride and the adamantane-like compounds $(MeSi)_4E_6$ (E = S, Se):

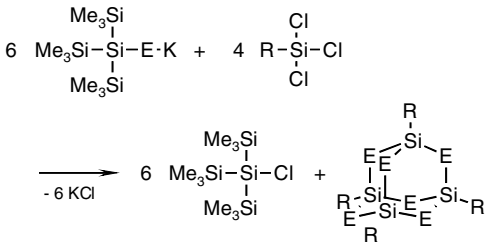

(4)

In case of reactions with R_2SiCl_2 the trimeric cyclic chalcogenides $(R_2SiE)_3$ have been observed along with hypersilyl chloride. The amount of these by-products decreases from the trichloro- to the dichlorosilanes and with increasing size of the organyl substituents.

These side reactions can be minimized by low reaction temperatures (−30 °C) and unpolar solvents, i.e. reactions with suspensions of $(Me_3Si)_3SiEK$ in hexane.

Surprisingly, such side reactions can hardly be observed in case of reactions with silicon tetrachloride.

All products have been characterized by multinuclear NMR spectroscopy. As one example a ^{29}Si NMR spectrum of $[(Me_3Si)_3SiSe]_2SiPhMe$ is shown in Fig. 1.

The NMR data are summarized in Tables 1 and 2.

As can be seen from Fig. 2, the ^{29}Si NMR signals of the central atoms of the hypersilyl units are shifted to

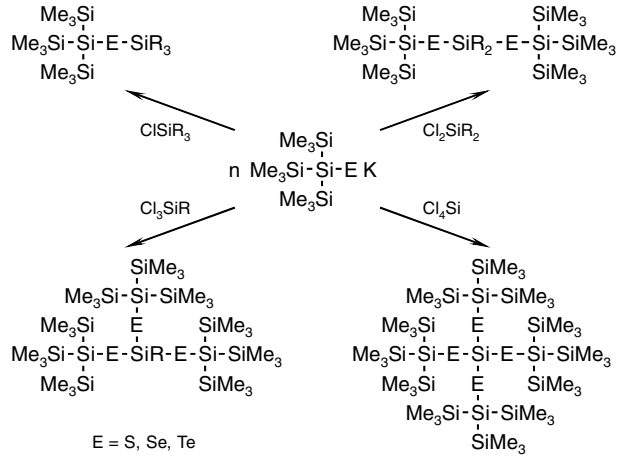

Scheme 2. Preparation of organosilicon hypersilylchalcogenolates.

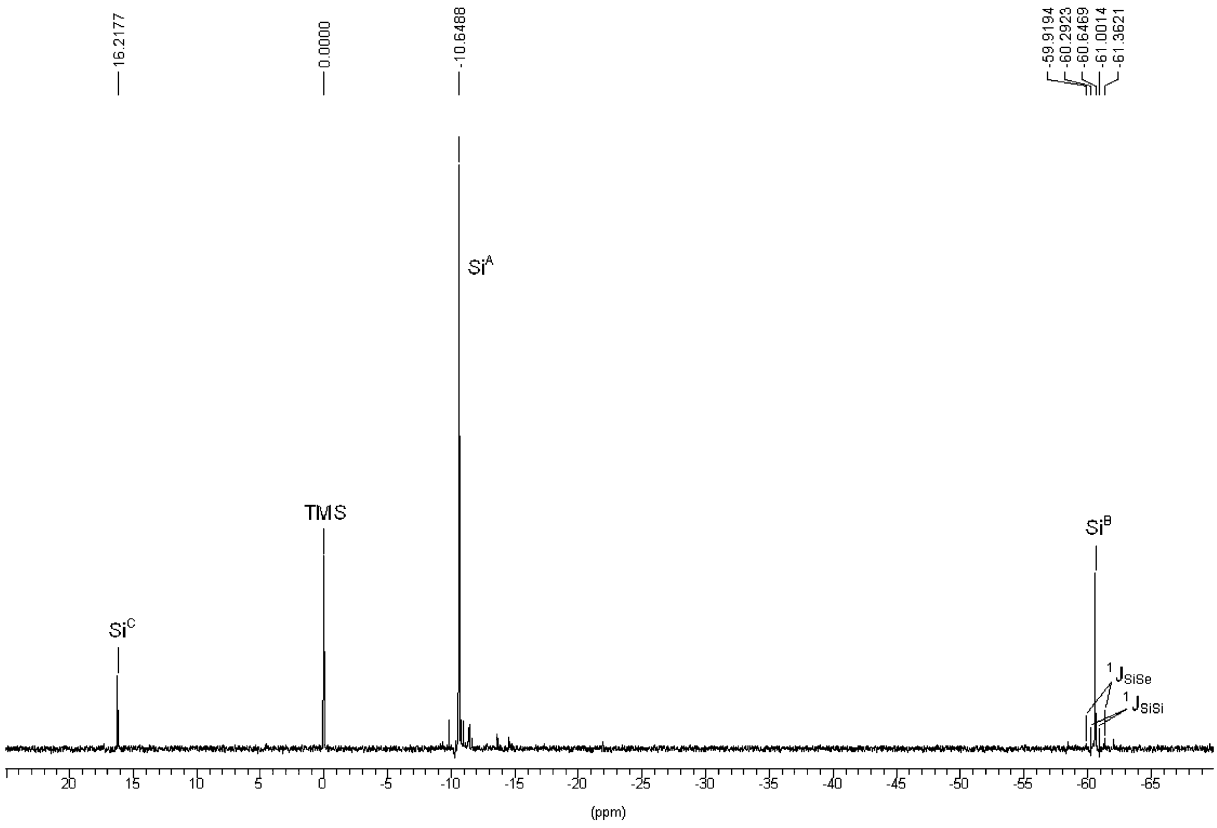

Fig. 1. ^{29}Si NMR spectrum of $[(Me_3Si^A)_3Si^BSe]_2Si^CPhMe$.

lower field with increasing number of hypersilylchalcogeno units and, to a lower extend, by increasing number of phenyl substituents. A multiple linear regression on the ^{29}Si NMR chemical shifts of Si^B yields the equations:

$E = S$:

$\delta^B_{Si} = -62.64\ \text{ppm} + 3.91\ \text{ppm} \cdot A + 1.17\ \text{ppm} \cdot B$ with $r = 0.979$

$E = Se$:

$\delta^B_{Si} = -74.68\ \text{ppm} + 5.73\ \text{ppm} \cdot A + 1.65\ \text{ppm} \cdot B$ with $r = 0.984$

$E = Te$:

$\delta^B_{Si} = -107.66\ \text{ppm} + 7.07\ \text{ppm} \cdot A + 1.43\ \text{ppm} \cdot B$ with $r = 0.999$

A is the number of $ESi(SiMe_3)_3$ units at Si^C and B is the number of phenyl groups at Si^C.

The dependence of the ^{29}Si NMR signals of the central silicon atom (Si^C) on the number of hypersilylchalcogeno units as well as phenyl substituents is shown in Fig. 3. As frequently described for other series $SiX_{4-x}Y_x$ a nonlinear "sagging" pattern is observed for E = S and Se while for E = Te further deviations occur. The exchange of methyl by phenyl substituents results in most cases in a high field shift of up to 10 ppm.

More instructive is a comparison of the data with those of the related chalcogenobutyl derivatives $Me_{4-x}Si(EBu)_x$ (E = S [45], Se [46], Te [47]) where the silicon atoms have the same first coordinations sphere. As can be seen from Fig. 4 the ^{29}Si NMR chemical shifts are almost identical for $x = 1$. For $x = 2$ the hypersilylthio and hypersilylseleno substitued silanes show additional low field shifts in respect to $Me_2Si(EBu)_2$ while the opposite effect is observed for E = Te. For $x = 3$ and 4 increasing high field shifts in respect to $MeSi(EBu)_3$ or $Si(EBu)_4$, respectively, are observed. Again, for E = Te the opposite, an increasing low field effect occurs.

These differences in general can be attributed to changes in bond angles (especially at the chalcogen atoms, see below) and bond lengths due to the increasing number of bulky hypersilyl units in the molecules.

The ^{77}Se and ^{125}Te NMR chemical shifts parallel the observation made for Si^B. With increasing number of hypersilylchalcogeno units δ_{Se} and δ_{Te} are shifted to lower field, in average δ_{Se} by 96 ppm per $SeSi(SiMe_3)_3$ unit and δ_{Te} by 202 ppm per $TeSi(SiMe_3)_3$ unit, see Figs. 5 and 6.

Also, the coupling constants $^1J_{Si^CSe}$ and $^1J_{Si^CTe}$ increase with the number of $ESi(SiMe_3)_3$ units at Si^C. This

Table 1
^{29}Si, ^{77}Se and ^{125}Te NMR data (Hz, ppm) of hypersilylchalcogenosubstituted silanes $[(Me_3Si)_3SiE]_xSiR_{4-x}$ (E = S, Se, Te; R = Me, Ph) and $[(Me_3Si)_3SiSe]_2SiPhCl$

Compound	δ_E	δ_{Si^A}	$^1J_{Si^ASi^B}$	δ_{Si^B}	$^1J_{Si^BE}$	δ_{Si^C}	$^1J_{Si^CE}$
$(Me_3Si^A)_3Si^BSSi^CMe_3$	–	–11.2	60.6	–58.0	–	15.6	–
$(Me_3Si^A)_3Si^BSSi^CMe_2Ph$	–	–11.1	60.3	–58.4	–	8.1	–
$(Me_3Si^A)_3Si^BSSi^CMePh_2$	–	–10.8	59.3	–57.7	–	2.0	–
$(Me_3Si^A)_3Si^BSSi^CPh_3$	–	–10.5	57.8	–54.5	–	–4.0	–
$[(Me_3Si^A)_3Si^BS]_2Si^CMe_2$	–	–10.4	58.8	–54.4	–	30.4	–
$[(Me_3Si^A)_3Si^BS]_2Si^CPhMe$	–	–10.2	61.2	–53.0	–	20.0	–
$[(Me_3Si^A)_3Si^BS]_2Si^CPh_2$	–	–10.0	57.4	–51.9	–	9.9	–
$[(Me_3Si^A)_3Si^BS]_3Si^CMe$	–	–10.0	61.2	–51.6	–	25.3	–
$[(Me_3Si^A)_3Si^BS]_3Si^CPh$	–	–9.9	58.8	–50.2	–	14.7	–
$[(Me_3Si^A)_3Si^BS]_4Si^C$	–	–9.5	55.2	–46.8	–	5.9	–
$(Me_3Si^A)_3Si^BSeSi^CMe_3$	–502	–11.6	58.8	–69.0	123.4	11.1	124.9
$(Me_3Si^A)_3Si^BSeSi^CMe_2Ph$	–502	–11.6	58.3	–68.0	122.0	4.9	132.2
$(Me_3Si^A)_3Si^BSeSi^CMePh_2$	–508	–11.5	57.8	–67.4	121.5	–0.2	
$(Me_3Si^A)_3Si^BSeSi^CPh_3$	–502	–10.9	55.9	–63.1	122.0	–3.6	
$[(Me_3Si^A)_3Si^BSe]_2Si^CMe_2$	–412	–10.8	56.9	–61.8	114.6	25.7	164.3
$[(Me_3Si^A)_3Si^BSe]_2Si^CPhMe$	–417	–10.6	56.4	–60.6	114.7	16.2	180.1
$[(Me_3Si^A)_3Si^BSe]_2Si^CPh_2$	–427	–10.5	55.8	–59.3	117.0	8.0	188.3
$[(Me_3Si^A)_3Si^BSe]_3Si^CMe$	–310	–10.5	55.4	–58.0	117.1	8.6	193.4
$[(Me_3Si^A)_3Si^BSe]_3Si^CPh$	–302	–10.3		–56.6		–0.3	196.5
$[(Me_3Si^A)_3Si^BSe]_4Si^C$	–213	–9.8	54.4	–51.9	115.0	–21.2	235.0
$(Me_3Si^A)_3Si^BTeSi^CMe_3$	–1076	–11.9	56.4	–100.5	288.7	–7.6	318.8
$(Me_3Si^A)_3Si^BTeSi^CMe_2Ph$	–1067	–11.6	56.4	–99.1	286.7	–12.6	338.2
$(Me_3Si^A)_3Si^BTeSi^CMePh_2$	–1060	–11.3	56.8	–98.3	285.7	–14.0	356.6
$(Me_3Si^A)_3Si^BTeSi^CPh_3$	–1055	–11.0	54.0	–96.1	292.5	–12.8	
$[(Me_3Si^A)_3Si^BTe]_2Si^CMe_2$	–873	–11.4	54.4	–93.6	294.5	–44.6	404.3
$[(Me_3Si^A)_3Si^BTe]_2Si^CPhMe$	–853	–11.1	54.4	–91.8	295.9	–47.4	419.9
$[(Me_3Si^A)_3Si^BTe]_2Si^CPh_2$	–834	–10.8	53.9	–90.6		–41.6	
$[(Me_3Si^A)_3Si^BTe]_3Si^CMe$	–682	–10.6	53.0	–86.4	280.9	–58.5	
$[(Me_3Si^A)_3Si^BTe]_3Si^CPh$	–657	–10.4	53.7	–84.9	283.3	–62.1	
$[(Me_3Si^A)_3Si^BTe]_4Si^C$	–468	–9.9	52.0	–79.6	269.7	–112.5	
$[(Me_3Si^A)_3Si^BSe]_2Si^CPhCl$	–339	–10.0	53.4	–55.1	109.8	3.0	214.5

is in accordance with the general observation that coupling constants $^1J_{SiX}$ increase with increasing number of electron withdrawing substituents at silicon.

In case of $Ph_2Si[TeSi(SiMe_3)_3]_2$ (**1**) single crystals of the compound have been obtained from a hexane solution and were suitable for a crystal structure analysis. The result is shown in Fig. 7.

Important bond lengths and angles of **1** are summarized in Table 3. The Si–Te bond lengths correspond to single bonds, however, the Si–Te bonds at Si1 are in average 0.05 Å shorter than the bonds Te1–Si2 and Te2–Si3. This is in accordance with the general observation that in organosilicon chalcogenides the Si–E bond lengths decrease with increasing number of chalcogen substituents at silicon. The relatively large bond angles Si–Te–Si, which even exceed the tetrahedral angle of 109.5°, reflect the steric crowding due to the presence of two bulky hypersilyl units. For comparison Si–Te–Si bond angles in the adamantane-like compound $(H_2C)_2(SiMe)_4Te_4$ [23] are 93.6–94.2° or 100.6–102.4° in cyclic $(Ph_2SiTe)_3$ [48]. In both compounds the Si–Te–Si units are part of six-membered rings.

If $PhSiCl_3$ is reacted with 1.5 equivalents of $(Me_3Si)_3SiSeK$ besides some residual $PhSiCl_3$ the partially substituted compound $[(Me_3Si)_3SiSe]_2SiPhCl$ (**2**) is observed. The NMR data of this product are given in Tables 1 and 2. In comparison with the threefold substituted compound $[(Me_3Si)_3SiSe]_3SiPh$ the remaining more electronegative chlorine substituent at Si^C causes a significant low field shift of the ^{77}Se NMR signal as well as an increase of the coupling constant $^1J_{Si^CSe}$. See Tables 5 and 6.

A crystal structure analysis of **2** has been carried out, the molecular structure is shown in Fig. 8.

This is the first crystal structure of a compound where a silicon atom is bond to both, selenium and chlorine. Due to the presence of the electron withdrawing chlorine atom in **2** the bond lengths Si–Se at Si1 are in average 0.08 Å shorter than the Si–Se bonds at Si2 and Si6. This is also reflected by the difference in the values of the coupling constants $^1J_{Si^BSe}$ of 109.8 Hz and $^1J_{Si^CSe}$ of 214.5 Hz.

Again, the relatively large bond angles at the selenium atoms of 109.9° and 114.1° are proof of the steric

Table 2
^{13}C and ^{1}H NMR data (Hz, ppm) of hypersilylchalcogenosubstituted silanes

Compound	δ_{C^A}	δ_{C^C}	$\delta_{C^{Ph}}$				δ_{H^A}	δ_{H^C}	$\delta_{H^{Ph}}$	
			ipso	*ortho*	*meta*	*para*			*o*	*m + p*
$(Me_3Si^A)_3Si^BSSi^CMe_3$	0.87	4.57	–	–	–	–	0.209	0.355	–	–
$(Me_3Si^A)_3Si^BSSi^CMe_2Ph$	0.79	3.38	139.4	133.8	127.7	129.4	0.183	0.550	7.61	7.2–7.5
$(Me_3Si^A)_3Si^BSSi^CMePh_2$	0.67	2.62	137.9	134.7	127.7	129.4	0.161	0.793	7.59	7.2–7.4
$(Me_3Si^A)_3Si^BSSi^CPh_3$	0.71	–	135.5	135.9	127.7	129.8	0.070	–	7.75	7.2–7.5
$[(Me_3Si^A)_3Si^BS]_2Si^CMe_2$	0.82	8.75	–	–	–	–	0.270	0.701	–	–
$[(Me_3Si^A)_3Si^BS]_2Si^CPhMe$	1.05	7.86	137.1	133.8	128.2	130.8	0.234	0.902	7.77	7.1–7.5
$[(Me_3Si^A)_3Si^BS]_2Si^CPh_2$	1.00	–	135.9	134.7	128.2	130.9	0.177	–	7.74	7.3–7.6
$[(Me_3Si^A)_3Si^BS]_3Si^CMe$	1.07	13.1	–	–	–	–	0.280		–	–
$[(Me_3Si^A)_3Si^BS]_3Si^CPh$	1.18	–	138.6	134.6	128.3	131.9	0.195	–	7.87	7.1–7.4
$[(Me_3Si^A)_3Si^BS]_4Si^C$	1.20	–	–	–	–	–	0.298	–	–	–
$(Me_3Si^A)_3Si^BSeSi^CMe_3$	0.98	5.04	–	–	–	–	0.254	0.462	–	–
$(Me_3Si^A)_3Si^BSeSi^CMe_2Ph$	0.94	3.86	139.2	133.9	127.7	129.4	0.205	0.666	7.5	7.2–7.4
$(Me_3Si^A)_3Si^BSeSi^CMePh_2$	0.89	2.33	137.7	134.9	127.8	129.5	0.176	0.803	7.60	7.1–7.3
$(Me_3Si^A)_3Si^BSeSi^CPh_3$	0.97	–	135.6	136.1	127.8	129.8	0.085	–	7.76	7.1–7.4
$[(Me_3Si^A)_3Si^BSe]_2Si^CMe_2$	1.04	9.17	–	–	–	–	0.293	0.845	–	–
$[(Me_3Si^A)_3Si^BSe]_2Si^CPhMe$	0.99	8.55		133.5	127.0	130.6	0.227	1.024	7.78	7.2–7.5
$[(Me_3Si^A)_3Si^BSe]_2Si^CPh_2$	0.96		135.8	134.5	127.9	130.7	0.183	–	7.76	7.2–7.6
$[(Me_3Si^A)_3Si^BSe]_3Si^CMe$	1.15	13.20	–	–	–	–	0.291	1.228	–	–
$[(Me_3Si^A)_3Si^BSe]_3Si^CPh$	1.16	–	138.8	134.2	127.9	130.8	0.217	–	7.87	7.3–7.5
$[(Me_3Si^A)_3Si^BSe]_4Si^C$	1.21	–	–	–	–	–	0.306	–	–	–
$(Me_3Si^A)_3Si^BTeSi^CMe_3$	1.15	6.22	–	–	–	–	0.270	0.604	–	–
$(Me_3Si^A)_3Si^BTeSi^CMe_2Ph$	1.26	4.86	138.9	133.7	127.7	129.4	0.219	0.850	7.60	7.1–7.3
$(Me_3Si^A)_3Si^BTeSi^CMePh_2$	1.36	2.68	137.1	134.9	127.8	129.6	0.164	1.153	7.67	7.2–7.5
$(Me_3Si^A)_3Si^BTeSi^CPh_3$	1.41	–	135.4	136.4	127.8	129.8	0.117	–	7.74	7.1–7.3
$[(Me_3Si^A)_3Si^BTe]_2Si^CMe_2$	1.75	11.23	–	–	–	–	0.298	0.975	–	–
$[(Me_3Si^A)_3Si^BTe]_2Si^CPhMe$	1.48	8.97	138.3	134.5	127.6	129.8	0.172	1.324	7.77	7.2–7.4
$[(Me_3Si^A)_3Si^BTe]_2Si^CPh_2$	1.56	–	135.7	136.4	127.6	130.0	0.106	–	7.91	7.2–7.4
$[(Me_3Si^A)_3Si^BTe]_3Si^CMe$	1.69	16.06	–	–	–	–	0.307	1.620	–	–
$[(Me_3Si^A)_3Si^BTe]_3Si^CPh$	1.59	–		133.8	127.7	130.6	0.189	–	7.89	7.2–7.5
$[(Me_3Si^A)_3Si^BTe]_4Si^C$	1.71	–	–	–	–	–	0.328	–	–	–
$[(Me_3Si^A)_3Si^BSe]_2Si^CPhCl$	1.05	–	131.8	133.5	128.2	131.7	0.278	–	7.85	7.3–7.5

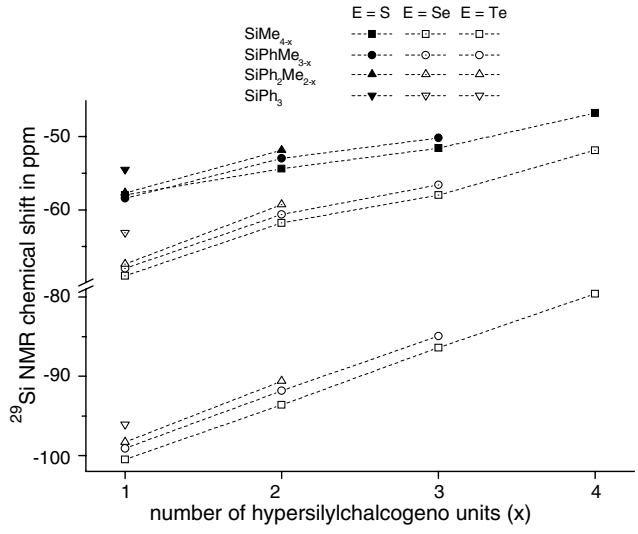

Fig. 2. ^{29}Si NMR chemical shifts of Si^B as a function of the number of hypersilylchalcogeno units at the central silicon atom (Si^C) for E = S, Se, Te and different numbers of phenyl substituents at Si^C.

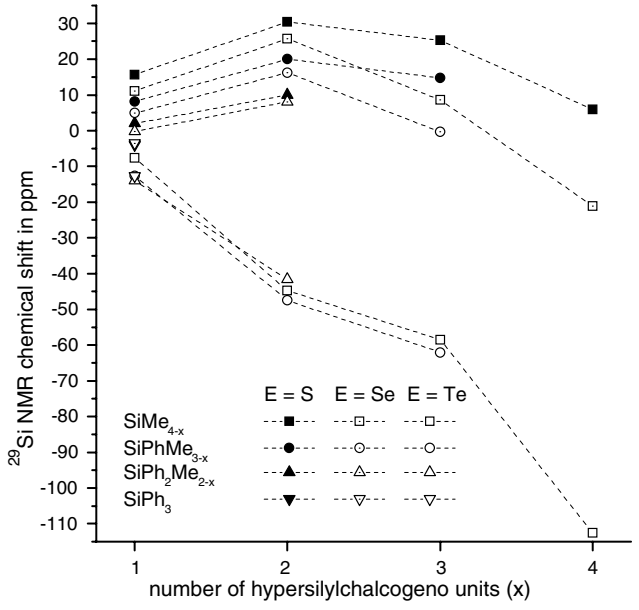

Fig. 3. ^{29}Si NMR chemical shifts of Si^C as a function of the number of hypersilylchalcogeno units at the central silicon atom (Si^C) for E = S, Se, Te and different numbers of phenyl substituents at Si^C.

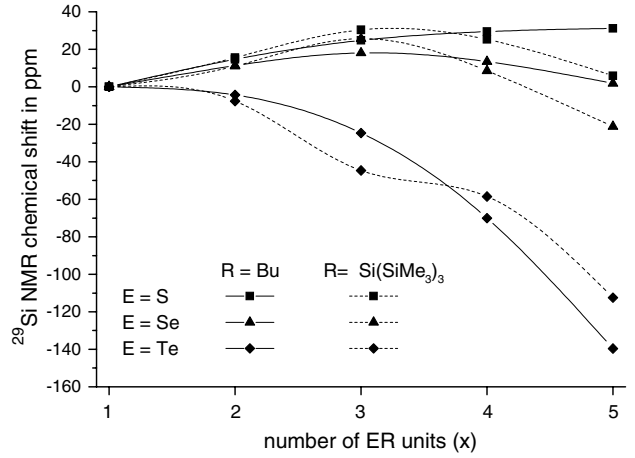

Fig. 4. ^{29}Si NMR chemical shifts in $Me_{4-x}Si(ER)_x$ ($x = 0 - 4$; E = S, Se, Te; R = *n*-Bu, $Si(SiMe_3)_3$.

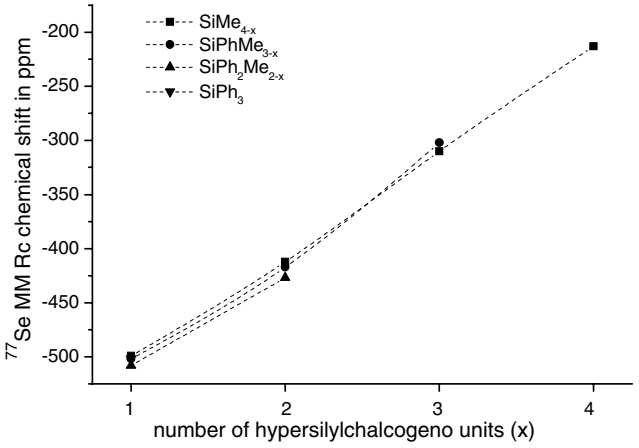

Fig. 5. ^{77}Se NMR chemical shifts in $[(Me_3Si^A)_3Si^BSe]_xSi^CR_{4-x}$ (R = Me, Ph) as a function of the number of hypersilylseleno units (x) and different numbers of phenyl substituents at Si^C.

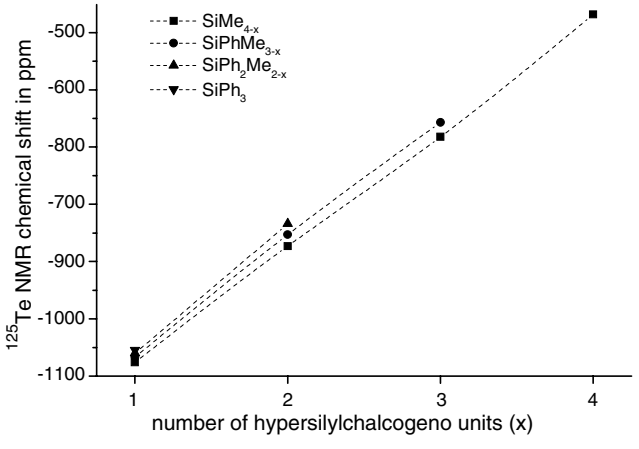

Fig. 6. ^{125}Te NMR chemical shifts in $[(Me_3Si^A)_3Si^BTe]_xSi^CR_{4-x}$ (R = Me, Ph) as a function of the number of hypersilyltelluro units (x) and different numbers of phenyl substituents at Si^C.

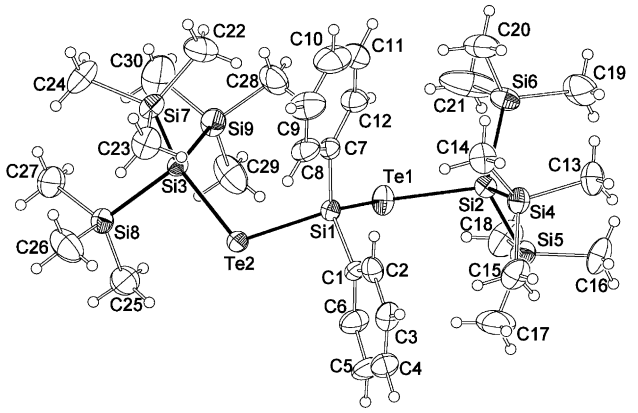

Fig. 7. Molecular structure of $[(Me_3Si)_3SiTe]_2SiPh_2$ (**1**).

Table 3
Selected bond lengths and bond angles of $[(Me_3Si)_3SiTe]_2SiPh_2$

Bond length (Å)	
Si1–Te1	2.501(2)
Si1–Te2	2.500(2)
Si2–Te1	2.555(2)
Si3–Te2	2.538(2)
Si2–Si4	2.343(3)
Si2–Si5	2.353(3)
Si2–Si6	2.351(3)
Si3–Si7	2.357(3)
Si3–Si9	2.346(3)
Si3–Si8	2.368(3)
Si1–C1	1.873(6)
Si1–C7	1.872(7)
Bond angle (°)	
Te1–Si1–Te2	104.71(7)
C1–Si1–C7	110.4(3)
Si1–Te1–Si2	111.91(7)
Si1–Te2–Si3	113.40(6)
Te1–Si2–Si	100.89(9)–118.02(10)
Te2–Si3–Si	96.61(8)–114.17(10)
Si–Si2–Si	109.17(10)–111.78(11)
Si–Si3–Si	109.75(12)–114.38(11)
Torsion angle (°)	
Si2–Te1–Si1–Te2	−168.68
Si3–Te2–Si1–Te1	−78.22

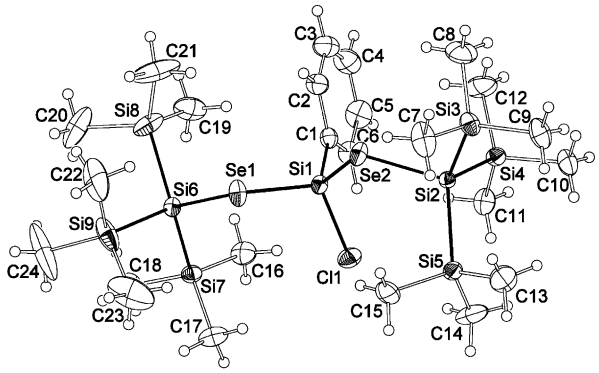

Fig. 8. Molecular structure of $[(Me_3Si)_3SiSe]_2SiPhCl$ (**2**).

crowding which is reduced by an expansion of these bond angles (see Table 4).

2.2. Hypersilylchalcogenolate derivatives of disilanes

The successful reaction of a whole series of organochlorosilanes with potassium hypersilylchalcogenolates tempted us to extend these investigations to reactions with methylchlorodisilanes.

Treatment of chloropentamethyldisilane and 1,2-dichlorotetramethyldisilane with potassium hypersilylchalcogenolates yielded the expected mono- and bis-hypersilylchalcogeno substituted disilanes:

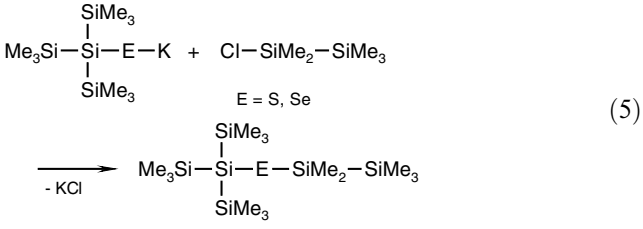

(5)

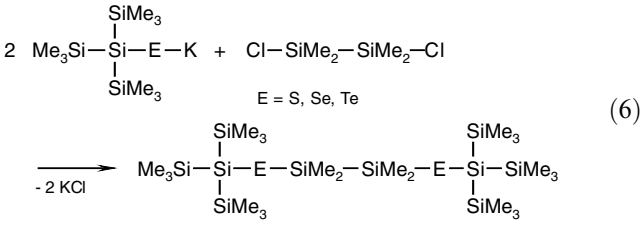

(6)

Table 4
Selected bond lengths and bond angles of $[(Me_3Si)_3SiSe]_2SiPhCl$

Bond length (Å)	
Si1–Cl1	2.066(1)
Si1–Se1	2.2417(9)
Si1–Se2	2.2556(8)
Si2–Se2	2.3237(8)
Si6–Se1	2.3281(9)
Si2–Si3	2.3557(12)
Si2–Si4	2.3467(11)
Si2–Si5	2.3613(11)
Si6–Si7	2.3433(12)
Si6–Si8	2.3489(13)
Si6–Si9	2.3413(13)
Si1–C1	1.859(3)
Bond angle (°)	
Se1–Si1–Se2	97.21(3)
Se1–Si1–Cl1	111.26(5)
Se2–Si1–Cl1	112.09(4)
Si1–Se2–Si2	109.94(3)
Si1–Se1–Si6	114.12(3)
Se2–Si2–Si	94.64(4)–114.86(4)
Se1–Si6–Si	95.07(4)–114.88(4)
Si–Si2–Si	110.71(4)–114.86(4)
Si–Si6–Si	109.97(6)–114.34(5)
Torsion angle (°)	
Si2–Se2–Si1–Se1	150.32
Si6–Se1–Si1–Se2	167.60

All products have been characterized by multinuclear NMR spectroscopy. Fig. 9 shows a ^{29}Si NMR spectrum of $(Me_3Si)_3SiSeSiMe_2SiMe_3$ as one example. Side reactions, i.e. formation of hypersilylchloride were not be observed in these reactions.

The NMR data of all prepared hypersilylchalcogenosubstituted disilanes are given in Tables 5 and 6. In comparison with $(Me_3Si^A)_3Si^BESi^CMe_3$ the ^{77}Se and ^{125}Te NMR signals are shifted to higher field by 20–30 ppm while the NMR data of the hypersilyl units remain almost unchanged (low field shift for Si^B of 1–3 ppm). As for the monohypersilylchalcogeno-substituted monosilanes the ^{29}Si NMR signals of Si^C and Si^D are close to the values reported for the corresponding chalcogenobutyl-substituted disilanes $BuESiMe_2SiMe_3$ (E = S, Se) and $BuESiMe_2SiMe_2EBu$ (E = S, Se, Te) [45–47].

$(Me_3Si)_3SiSeSiMe_2SiMe_2SeSi(SiMe_3)_3$ (**3**) has also been characterized by a crystal structure analysis, see Fig. 10. Due to a crystallographic centre of inversion at the central Si–Si bond the hypersilylseleno substituents are in an exact *anti* orientation (torsion angle Se1–Si3–Si3a–Se1a: 180.00°). Important bond lengths and angles are given in Table 7. Again, the bond angle at selenium is relatively large, e.g. in comparison with the cyclic six-membered ring compound $Se(SiMe_2SiMe_2)_2Se$ (∠Si–Se–Si: 105.14(3)°) [7].

2.3. Organosilicon heptasilanylthiolates $[(Me_3Si)_3Si(Me_3Si)_2SiS]_xSiMe_{4-x}$

The selective cleavage of terminal silicon–silicon bonds in highly branched oligosilanes by KO^tBu makes a pentakis(trimethylsilyl)disilanyl potassium species easily accessible [40,42].

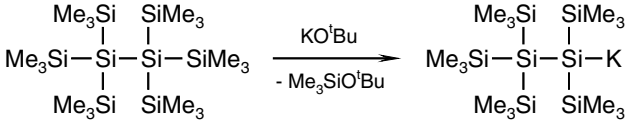

(7)

Subsequent reactions with elemental chalcogens as in Eq. (3) were only successful in the case of sulfur:

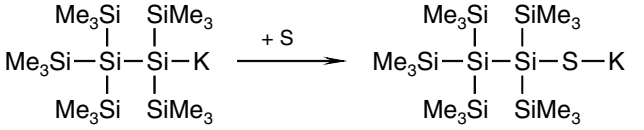

(8)

Reactions of the potassium pentakis(trimethylsilyl) disilanylthiolate with methylchlorosilanes led to the expected heptasilanylthiolate derivatives (Scheme 3).

In contrast to reactions with potassium hypersilylthiolate side reactions as shown in Eq. (4) could not be

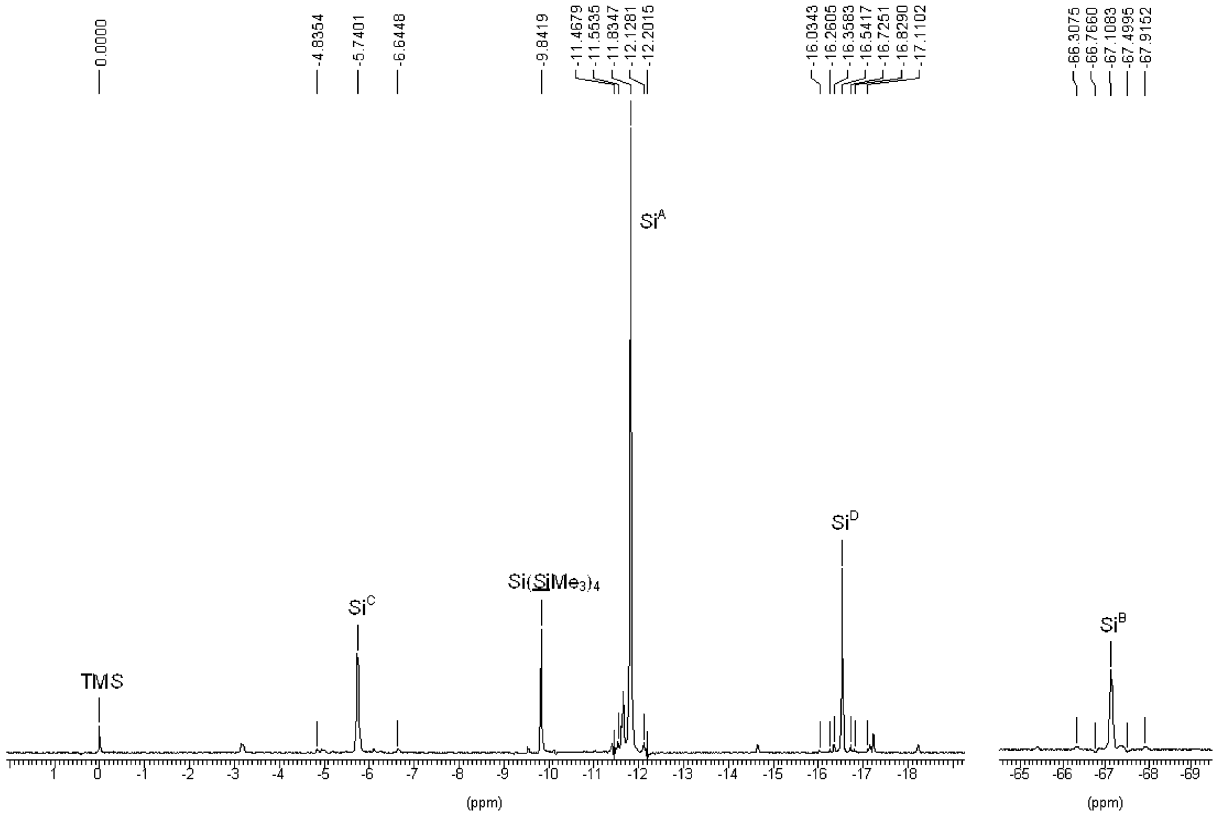

Fig. 9. ^{29}Si NMR spectrum of $(Me_3Si^A)_3Si^BSeSi^CMe_2Si^DMe_3$.

Table 5
^{29}Si, ^{77}Se and ^{125}Te NMR data (Hz, ppm) of hypersilylchalcogenosubstituted disilanes (E = S, Se, Te)

Compound	δ_E	δ_{Si^A}	δ_{Si^B}	$^1J_{Si^ASi^B}$	$^1J_{Si^BE}$	δ_{Si^C}	$^1J_{Si^CE}$	δ_{Si^D}
$(Me_3Si^A)_3Si^B-S-Si^CMe_2Si^DMe_3$	–	−11.3	−57.8	59.8	–	−0.8	–	−17.1
$[(Me_3Si^A)_3Si^B-S-Si^CMe_2-]_2$	–	−11.2	−56.5	59.3	–	−0.8	–	–
$(Me_3Si^A)_3Si^B-Se-Si^CMe_2Si^DMe_3$	−527	−11.8	−67.1	58.3	127.8	−5.7	143.8	−16.5
$[(Me_3Si^A)_3Si^B-Se-Si^CMe_2-]_2$	−523	−11.7	−65.4	57.3	126.8	−6.1	144.3	–
$[(Me_3Si^A)_3Si^B-Te-Si^CMe_2-]_2$	−1107	−11.8	−98.1	54.1	298.8	−28.8	367.9[a]	–

[a] $^2J_{Si^CTe}$: 70.4 Hz.

Table 6
^{1}H and ^{13}C NMR data (Hz, ppm) of hypersilylchalcogenosubstituted disilanes

Compound	δ_{C^A}	$^1J_{SiC}$	δ_{C^C}	δ_{C^D}	δ_{H^A}	δ_{H^C}	δ_{H^D}
$(Me_3Si^A)_3Si^BSSi^CMe_2Si^DMe_3$	0.78		2.44	−2.50	0.238	0.244	0.120
$\{[(Me_3Si^A)_3Si^BSSi^CMe_2\}$	0.76		2.14	–	0.235	0.466	–
$(Me_3Si^A)_3Si^BSeSi^CMe_2Si^DMe_3$	1.04	45.2	2.34	−2.40	0.249	0.494	0.139
$\{[(Me_3Si^A)_3Si^BSe]Si^CMe_2\}$	1.02	45.2	2.33	–	0.229	0.596	–
$\{[(Me_3Si^A)_3Si^BTe]Si^CMe_2\}$	1.33	45.9	2.53	–	0.272	0.762	–

observed here. This reflects the increased steric shielding of the larger oligosilanyl group and increased kinetic stability of the Si–S bond in the heptasilanylthiolate unit.

The NMR data of potassium pentakis (trimethylsilyl)disilanylthiolate and heptasilanylthiosubstituted silanes $[(Me_3Si)_3Si–Si(SiMe_3)_2S]_xSiMe_{4-x}$ are summarized in Tables 8 and 9.

A comparison with the NMR data of the hypersilylthiolate derivatives reveals that the substitution of one $SiMe_3$ unit in hypersilylthiolates by a hypersilyl unit $Si(SiMe_3)_3$ results in a low field shift of the ^{29}Si NMR signal of the silicon atom directly bound to sulfur of 6.5 (potassium thiolates) or 14–17 ppm (organosilicon thiolates), respectively.

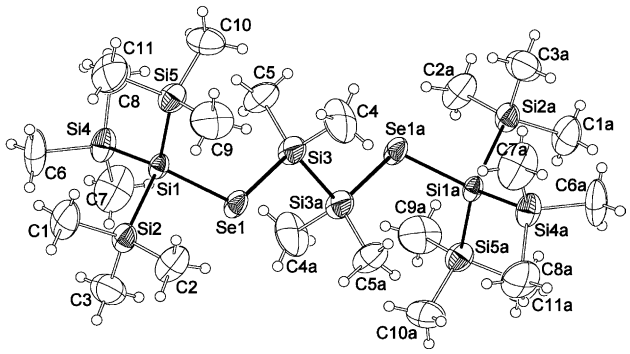

Fig. 10. Molecular structure of $[(Me_3Si)_3SiSeSiMe_2]_2$ (**3**).

Table 7
Selected bond lengths and bond angles of $[(Me_3Si)_3SiSeSiMe_2]_2$ (**3**)

Bond length (Å)	
Si3–Se1	2.259(2)
Si1–Se1	2.307(1)
Si3–Si3a	2.279(4)
Si1–Si2	2.349(2)
Si1–Si4	2.345(2)
Si1–Si5	2.343(3)
Bond angle (°)	
Si3a–Si3–Se1	103.08(13)
Si3–Se1–Si1	114.59(6)
Se1–Si1–Si	97.24(7)–113.55(8)
Si–Si1–Si	109.05(10)–113.45(9)
Torsion angle (°)	
Se1–Si3–Si3a–Se1a	180.00
Si1–Se1–Si3–Si3a	−154.14

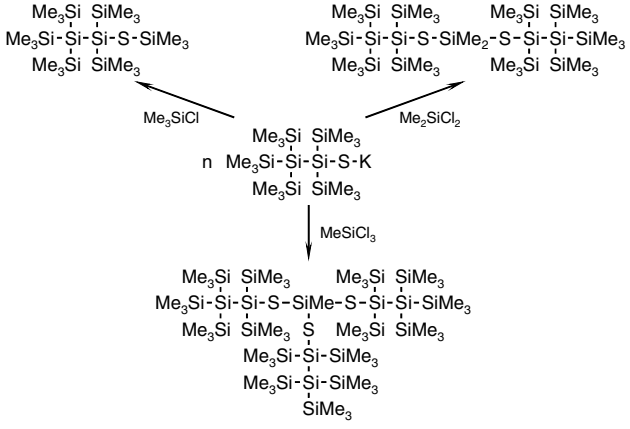

Scheme 3. Preparation of organosilicon heptasilanylthiolates.

Fig. 11 shows a comparison of the ^{29}Si NMR chemical shifts in $Me_{4-x}Si(SR)_x$ (SR = $SSi(SiMe_3)_3$ and $SSi(SiMe_2)_2Si(SiMe_3)_3$). While for $x = 1$ the chemical shifts are almost identical, for $x = 2$ and 3 an increasing additional high field shift for the heptasilanylthiolate derivatives can be observed as consequence of the larger steric demand of the heptasilanylthiolate units.

3. Experimental

3.1. NMR and GC/MS measurements

All NMR spectra were recorded on a Bruker DPX 400 in $CDCl_3$ solution and TMS as internal standard for ^{1}H, ^{13}C and ^{29}Si. In order to get a sufficient signal to noise ratio of ^{29}Si NMR spectra for obtaining $^1J_{SiC}$, $^1J_{SiSi}$, $^1J_{SiSe}$ or $^1J_{SiTe}$ satellites ^{29}Si INEPT spectra were also recorded. ^{77}Se and ^{125}Te NMR spectra were obtained using an IGATED pulse program.

External $CDCl_3$ solutions of Ph_2Se_2 (δ_{Se}: 460 ppm [49]) and Ph_2Te_2 (δ_{Te}: 422 ppm [50]) were used as standards for ^{77}Se and ^{125}Te.

Mass spectra were measured on a Hewlett–Packard 5971 (ionization energy: 70 eV, column: 30 m × 0.25 mm × 0.25 μm, phenylmethylpolysiloxane, column temperature: 80 °C (3 min)/20 K/min/200 °C, flow: He 0.5 mL/min).

3.2. Crystal structure analyses

X-ray structure analysis measurements of **1** and **3** were performed on a Rigaku AFC7 with Mercury CCD, while a Bruker Smart CCD was used for **2**. Crystal data of **1**–**3** as well as data collection and refinement details are given in Table 10.

The unit cell of **2** was determined with the program SMART [51]. For data integration and refinement of the unit cell the program SAINT [51] was used. The space group was determined using the program XPREP [51]. All data were corrected for absorption using SADABS [52]. For the data collection, unit cell refinement and data reduction of **1** and **3** the program package CRYSTAL CLEAR [53] was used. The structures were solved using direct methods (SIR-97 [54]), refined

Table 8
^{29}Si NMR data (Hz, ppm) of potassium pentakis(trimethylsilyl)disilanylthiolate and heptasilanylthiosubstituted silanes $[(Me_3Si)_3Si–Si(SiMe_3)_2S]_xSiMe_{4-x}$

Compound	δ_{Si^A}	$^1J_{Si^ASi^B}$	δ_{Si^B}	δ_{Si^C}	δ_{Si^D}	$^1J_{Si^CSi^D}$	δ_{Si^E}
$(Me_3Si^A)_3Si^BSi^C(Si^DMe_3)_2SK$[a]	−9.8	50.1	−128.2	−53.7	−17.2	71.2	–
$[(Me_3Si^A)_3Si^BSi^C(Si^DMe_3)_2S]Si^EMe_3$	−9.1	51.6[b]	−118.1	−44.5	−11.3	58.9	15.3
$[(Me_3Si^A)_3Si^BSi^C(Si^DMe_3)_2S]_2Si^EMe_2$	−8.9	50.5	−117.6	−40.0	−10.1	57.8	28.6
$[(Me_3Si^A)_3Si^BSi^C(Si^DMe_3)_2S]_3Si^EMe$	−8.8	50.1	−117.1	−34.5	−9.1		17.5

[a] In THF solution.
[b] $^1J_{Si^BSi^C}$: 29.1 Hz.

Table 9
^{13}C and ^{1}H NMR data (Hz, ppm) of potassium pentakis(trimethylsilyl)disilanylthiolate and heptasilanylthiosubstituted silanes $[(Me_3Si)_3Si–Si(SiMe_3)_2S]_xSiMe_{4-x}$

Compound	δ_{C^A}	$^1J_{Si^AC}$	δ_{C^D}	$^1J_{Si^DC}$	δ_{C^E}	δ_{H^A}	δ_{H^D}	δ_{H^E}
$(Me_3Si^A)_3Si^BSi^C(Si^DMe_3)_2SK$[a]	4.05	43.0	1.40		–	0.399	0.281	–
$[(Me_3Si^A)_3Si^BSi^C(Si^DMe_3)_2S]Si^EMe_3$	4.12	44.5	2.36	45.2	4.89	0.295	0.308	0.354
$[(Me_3Si^A)_3Si^BSi^C(Si^DMe_3)_2S]_2Si^EMe_2$	4.04	44.7	2.35		8.41	0.299	0.342	0.712
$[(Me_3Si^A)_3Si^BSi^C(Si^DMe_3)_2S]_3Si^EMe$	4.10		2.45		11.86	0.313	0.378	1.015

[a] In THF solution.

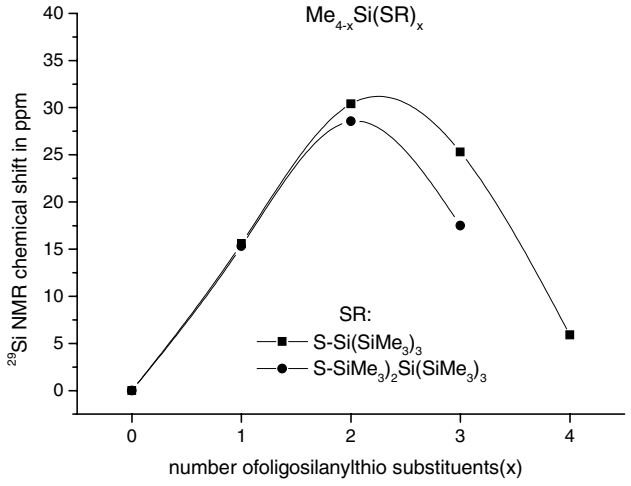

Fig. 11. Comparison of the ^{29}Si NMR chemical shifts in $Me_{4-x}Si(SR)_x$ (SR = S–$Si(SiMe_3)_3$ and S–$Si(SiMe_2)_2$–$Si(SiMe_3)_3$).

using least-squares-methods (SHELX-97 [55]) and drawn using DIAMOND [56]. The ellipsoides at the nonhydrogen atoms are shown at the 30% probability level.

3.3. Starting materials

Sulfur, selenium, tellurium, KO^{t}Bu and all organochlorosilanes $R_{4-x}SiCl_x$ (R = Me, Ph, Me/Ph; x = 1–4) were commercially available. $ClSi_2Me_5$ [57], $ClMe_2Si–SiMe_2Cl$ [58] and $Si_2(SiMe_3)_6$ [40,59] have been prepared as described. THF solutions of potassium hypersilylchalcogenolates were obtained as reported in [44].

THF was distilled from sodium potassium alloy prior to use. Hexane was dried over KOH. All reactions were carried out under argon applying standard Schlenk techniques.

3.4. Synthesis of organosilicon hypersilylchalcogenolates (general procedure)

R_3SiCl (3.0 mmol), 3.0 mmol Me_5Si_2Cl, 1.5 mmol R_2SiCl_2, 1.5 mmol $ClMe_2Si–SiMe_2Cl$, 1.0 mmol $RSiCl_3$ or 0.75 mmol $SiCl_4$ (R = Me, Ph, Me/Ph) diluted in 1 mL hexane was added to THF solutions of potassium hyper ilylchalcogenolates prepared from $Si(SiMe_3)_4$ (1.0 g, 3.1 mmol), KO^{t}Bu (0.40 g, 3.6 mmol) and elemental chalcogen (3.1 mmol sulfur, selenium or tellurium) in THF (4 mL) [44]. After stirring over night the solvent was removed in vacuo. The residue was dissolved in 10 mL hexane, filtered from precipitated salts and the solvent removed.

$[(Me_3Si)_3SiSe]_2SiPhCl$ was prepared in a similar manner by slow addition of a THF solution of potassium hypersilylselenolate (3.1 mmol) to a solution of $PhSiCl_3$ (0.42 g, 2.0 mmol) in 1 mL hexane.

To reduce the formation of undesired by-products (hypersilyl chloride and organosilicon chalcogenides) the THF solutions of potassium hypersilylchalcogenolates were concentrated in vacuo and the residue suspended in hexane (6 mL). 1.5 mmol Me_2SiCl_2 or 1.0 mmol $MeSiCl_3$ diluted in 1 mL hexane was added to this suspension at −30 °C. After reacting over night the mixture was filtered and the solvent removed in vacuo.

$[(Me_3Si)_3SiE]_2SiPh_2$, $[(Me_3Si)_3SiE]_3SiPh$ and $(Me_3Si)_3SiESiMe_2SiMe_2ESi(SiMe_3)_3$ were obtained in crystalline form while the monosubstituted compounds $(Me_3Si)_3SiESiR_3$ and $Me_3Si)_3SiESi_2Me_5$ are viscous oils and the tetrasubstituted silanes $[(Me_3Si)_3SiE]_4Si$ show little tendency to crystallize.

Besides characterization by NMR spectroscopy some monosubstituted silanes could also be investigated by GC/MS.

$(Me_3Si)_3SiSSiMe_3$. GC/MS (*m/e*, rel. int.): 352 (M^+, 32), 337 (M^+ − Me, 8), 279 (Me_9Si_4S, 15), 264 (Me_8Si_4S, 3), 249 (Me_7Si_4S, 8), 191 (Me_5Si_3S, 42), 174 (Me_6Si_3, 19), 159 (Me_5Si_3, 10), 131 (Me_5Si_2, 23), 73 (Me_3Si, 100).

$(Me_3Si)_3SiSSiMe_2Ph$. GC/MS: 414 (M^+, 31), 399 (M^+ − Me, 8), 341 ($PhMe_8Si_4S$, 9), 264 (Me_8Si_4S, 10), 253 ($PhMe_4Si_3S$, 10), 249 (Me_7Si_4S, 11), 236 ($PhMe_5Si_3$, 40), 221 ($PhMe_4Si_3$, 23), 193 ($PhMe_4Si_2$, 20), 191 (Me_5Si_3S, 65), 177 (29), 162 (33), 135 ($PhMe_2Si$, 100), 131 (Me_5Si_2, 30), 73 (Me_3Si, 95).

$(Me_3Si)_3SiSSiMePh_2$. GC/MS: 476 (M^+, 16), 461 (M^+ − Me, 5), 403 ($Ph_2Me_7Si_4S$, 5), 326 ($PhMe_7Si_4S$, 5), 298 ($Ph_2Me_4Si_3$, 38), 283 ($Ph_2Me_3Si_3$, 8), 253 ($PhMe_4Si_3S$, 40), 239 (46), 238 ($PhMe_3Si_3S$, 33), 197 (Ph_2MeSi, 100), 191 (Me_5Si_3S, 36), 135 ($PhMe_2Si$, 77), 131 (Me_5Si_2, 31), 105 (PhSi, 18), 73 (Me_3Si, 86).

Table 10
Crystal data of **1**, **2** and **3** as well as data collection and refinement details

compound	**1**	**2**	**3**
Empirical formula	$C_{30}H_{64}Si_9Te_2$	$C_{24}H_{59}ClSe_2Si_9$	$C_{22}H_{66}Se_2Si_{10}$
Formula weight	932.82	793.89	769.55
Crystal shape	Block	Block	Block
Temperature (K)	295(2)	298(2)	295(2)
Crystal color	Yellow	Colorless	Colorless
Crystal size (mm^3)	$0.19 \times 0.15 \times 0.12$	$0.40 \times 0.30 \times 0.30$	$0.32 \times 0.31 \times 0.25$
Crystal system	Triclinic	Triclinic	Monoclinic
Space group	$P\bar{1}$	$P\bar{1}$	$C2/c$
Unit cell dimensions			
a (Å)	10.0818(5)	9.7773(5)	15.897(4)
b (Å)	15.4719(8)	13.9268(5)	16.1270(3)
c (Å)	17.5220(12)	17.0547(10)	18.0610(3)
α (°)	75.217(13)	82.210(10)	90
β (°)	72.003(13)	76.592(10)	94.045
γ (°)	72.821(13)	76.132(10)	90
Volume ($Å^3$); Z	2442.7(2); 2	2185.3(2); 2	4618.8(16); 4
Density (calc., g/cm^3)	1.268	1.207	1.106
Linear absorption coeff. (mm^{-1})	1.432	2.014	1.872
Scan method	φ scans	ω scans	φ scans
Absorption correction	Multiscan	Empirical	Multiscan
Measured reflections	28,511	44,161	13775
Independent reflections	6676	8912	13775
Observed reflections	5575	6814	11727
R_{int}	0.0665	0.0313	–
θ range for collection (°)	2.20–23.00	1.51–26.37	2.17–24.00
Index ranges	$-11 \leqslant h \leqslant 11$	$-11 \leqslant h \leqslant 12$	$-17 \leqslant h \leqslant 18$
	$-17 \leqslant k \leqslant 17$	$-16 \leqslant k \leqslant 17$	$-18 \leqslant k \leqslant 18$
	$-19 \leqslant l \leqslant 19$	$0 \leqslant l \leqslant 21$	$-20 \leqslant l \leqslant 20$
Completeness to θ_{max} (%)	98.4	99.7	99.5
Number of parameters	370	343	166
Final R_1/wR^2 $[I > 2\sigma(I)]$[a]	0.0719/0.1169	0.0392/0.0906	0.1007/0.2615
Final R_1/wR^2 (all data)[a]	0.0915/0.1218	0.0584/0.0993	0.1122/0.2700
Goodness-of-fit (S)[b] on F^2	1.360	1.028	1.106
H-locating and refining	Geom./mixed	Geom./mixed	Geom./mixed
Max./min. e-density ($e/Å^3$)	0.749/−0.508	0.964/−0.771	2.001/−0.805

[a] $R_1 = \sum(||F_o| - |F_c||)/\sum|F_o|$, $wR^2 = [\sum(w(F_o^2 - F_c^2)^2)/\sum(wF_o^2)]^{1/2}$, $w = 1/[\sigma^2(F_o^2) + (aP)^2 + bP]$, where $P = (F_o^2 + 2F_c^2)/3$.
[b] $S = [\sum w(F_o^2 - F_c^2)^2]/(n-p)^{1/2}$, n = number of reflections, p = parameters used.

$(Me_3Si)_3SiSeSiMe_3$. GC/MS: 400 (M^+, 19), 375 (M^+ − Me, 4), 327 (Me_9Si_4Se, 9), 312 (Me_8Si_4Se, 2), 297 (Me_7Si_4Se, 5), 239 (Me_5Si_3Se, 30), 174 (Me_6Si_3, 12), 159 (Me_5Si_3, 6), 131 (Me_5Si_2, 23), 73 (Me_3Si, 100).

$(Me_3Si)_3SiSeSiMe_2Ph$. GC/MS: 462 (M^+, 9), 447 (M^+ − Me, 1), 389 ($PhMe_8Si_4Se$, 3), 312 (Me_8Si_4Se, 1), 301 ($PhMe_4Si_3Se$, 5), 297 (Me_7Si_4Se, 5), 239 (Me_5Si_3Se, 27), 236 ($PhMe_5Si_3$, 40), 221 ($PhMe_4Si_3$, 10), 193 ($PhMe_4Si_2$, 8), 162 (19), 135 ($PhMe_2Si$, 100), 131 (Me_5Si_2, 32), 73 (Me_3Si, 99).

3.5. Synthesis of organosilicon pentakis(trimethylsilyl)-disilanylthiolates

3.5.1. Potassium pentakis(trimethylsilyl)disilanylthiolate

$Si_2(SiMe_3)_6$ (0.50 g, 1.0 mmol) was dissolved in THF (4 mL) and KO^{t}Bu (0.12 g, 1.05 mmol) was added. After stirring over night a ^{29}Si NMR spectrum of the THF solution revealed a complete conversion to $(Me_3Si^A)_3Si^B{-}Si^C(Si^DMe_3)_2K$ (δ_{Si}: −11.1 ppm (A), −129.0 ppm (B), −190.6 ppm (C), −6.5 ppm (D) and Me_3SiO^tBu. At −30 °C sulfur (32 mg, 1.0 mmol) was added under formation of $(Me_3Si)_3SiSi(SiMe_3)_2SK$ as checked by NMR (see Tables 8 and 9).

3.5.2. Organosilicon pentakis(trimethylsilyl)disilanylthiolates

Me_3SiCl (0.11 g, 1.0 mmol), Me_2SiCl_2 (64 mg, 0.5 mmol) or $MeSiCl_3$ (48 mg, 0.33 mmol) diluted in 1 mL hexane was added to a THF solution of potassium pentakis(trimethylsilyl)disilanylthiolate (1.0 mmol). After stirring over night the solvent was removed in vacuo. The residue was dissolved in 10 mL hexane, filtered from precipitated salts and the solvent removed.

Besides characterization by NMR spectroscopy the monosubstituted silane could also be investigated by GC/MS.

$(Me_3Si)_3SiSi(SiMe_3)_2SSiMe_3$. GC/MS (*m/e*, rel. int.): 526 (M^+, 2), 511 (M^+ − Me, 3), 453 ($Me_{15}Si_7S$, 1), 348

($Me_{12}Si_6$, 50), 275 (Me_9Si_5, 6), 191 (Me_5Si_3S, 8), 163 (Me_5Si_2S, 6), 131 (Me_5Si_2, 11), 73 (Me_3Si, 100).

4. Supplementary material

Crystallographic data for the structural analyses have been deposited at the Cambridge Crystallographic Data Centre as Supplementary Publication Nos. 252708 for **1**, 252709 for **2** and 252710 for **3**.

Copies of this information may be obtained free of charge from The Director, CCDC, 12 Union Road, Cambridge CB2 1EZ, UK (fax: +44-1223-336033; e-mail: deposit@ccdc.cam.ac.uk or www: http://www.ccdc.cam.ac.uk).

Acknowledgment

The authors thank the 'Deutsche Forschungsgemeinschaft' and the 'Fonds der Chemischen Industrie' for financial support.

References

[1] W.E. Schklower, Yu.T. Strutschkow, L.E. Guselnikow, W.W. Wolkowa, W.A. Awakyan, Z. Anorg. Allg. Chem. 501 (1983) 153.
[2] M. Haaf, A. Schmiedel, T.A. Schmedake, D.R. Powell, A.J. Millevolte, M. Denk, R. West, J. Am. Chem. Soc. 120 (1998) 12714.
[3] B. Gehrhus, P.B. Hitchcock, M.F. Lappert, J. Heinicke, R. Boese, D. Bläser, J. Organomet. Chem. 521 (1996) 211.
[4] M. Weidenbruch, L. Kirmaier, E. Kroke, W. Saak, Z. Anorg. Allg. Chem. 623 (1997) 1277.
[5] U. Herzog, H. Borrmann, Inorg. Chem. Commun. 6 (2003) 718.
[6] H. Nöth, H. Fußstetter, H. Pommerening, T. Taeger, Chem Ber. 113 (1980) 342.
[7] U. Herzog, G. Rheinwald, J. Organomet. Chem. 627 (2001) 23.
[8] D.L. Mayfield, R.A. Flath, L.R. Best, J. Org. Chem. 29 (1964) 2444.
[9] L. Pazdernik, F. Brisse, R. Rivest, Acta Cryst. B 33 (1977) 1780.
[10] M. Schmidt, H. Ruf, Z. Anorg. Allg. Chem. 321 (1963) 270.
[11] P. Boudjouk, S.R. Bahr, D.P. Thompson, Organometallics 10 (1991) 778.
[12] U. Wannagat, O. Brandstätter, Monatsh. Chem. 94 (1963) 1090.
[13] E. Hengge, H.G. Schuster, J. Organomet. Chem. 240 (1982) C65.
[14] U. Herzog, U. Böhme, E. Brendler, G. Rheinwald, J. Organomet. Chem. 630 (2001) 139.
[15] W. Wojnowski, B. Dręczewski, A. Herman, K. Peters, E.-M. Peters, H.G.v. Schnering, Angew. Chem. 97 (1985) 978.
[16] U. Herzog, U. Böhme, G. Rheinwald, J. Organomet. Chem. 627 (2001) 144.
[17] U. Herzog, G. Rheinwald, Organometallics 20 (2001) 5369.
[18] J. Peters, J. Mandt, M. Meyring, B. Krebs, Z. Kristallogr. 156 (1981) 90.
[19] A. Haas, R. Hitze, C. Krüger, K. Angermund, Z. Naturforsch. B 39 (1984) 890.
[20] J.C.J. Bart, J.J. Daly, J. Chem. Soc., Dalton Trans. (1975) 2063.
[21] S.R. Bahr, P. Boudjouk, Inorg. Chem. 31 (1992) 712.
[22] W. Ando, T. Kadowaki, A. Watanabe, N. Choi, Y. Kabe, T. Erata, M. Ishii, Nippon Kagaku Kaishi (1994) 214.
[23] U. Herzog, G. Rheinwald, J. Organomet. Chem. 628 (2001) 133.
[24] C. Ackerhans, H.W. Roesky, M. Noltemeyer, Organometallics 20 (2001) 1282.
[25] U. Herzog, U. Böhme, G. Roewer, G. Rheinwald, H. Lang, J. Organomet. Chem. 602 (2000) 193.
[26] S.P. Wuller, A.L. Seligson, G.P. Mitchell, J. Arnold, Inorg. Chem. 34 (1995) 4854.
[27] A.L. Seligson, J. Arnold, J. Am. Chem. Soc. 115 (1993) 8214.
[28] D.R. Cary, J. Arnold, Inorg. Chem. 33 (1994) 1791.
[29] C.P. Gerlach, V. Christou, J. Arnold, Inorg. Chem. 35 (1996) 2758.
[30] V. Christou, S.P. Wuller, J. Arnold, J. Am. Chem. Soc. 115 (1993) 10545.
[31] C.P. Gerlach, S.P. Wuller, J. Arnold, J. Chem. Soc., Chem. Commun. (1996) 2565.
[32] D.E. Gindelberger, J. Arnold, Inorg. Chem. 32 (1993) 5813.
[33] P.J. Bonasia, J. Arnold, Inorg. Chem. 31 (1992) 2508.
[34] P.J. Bonasia, V. Christou, J. Arnold, J. Am. Chem. Soc. 115 (1993) 6777.
[35] H. Gilman, J.M. Holmes, C.L. Smith, Chem. Ind. (London) (1965) 848.
[36] G. Becker, K.W. Klinkhammer, S. Lartiges, P. Böttcher, W. Poll, Z. Anorg. Allg. Chem. 613 (1992) 7.
[37] B.O. Dabbousi, P.J. Bonasia, J. Arnold, J. Am. Chem. Soc. 113 (1991) 3186.
[38] P.J. Bonasia, D.E. Gindelberger, B.O. Dabbousi, J. Arnold, J. Am. Chem. Soc. 114 (1992) 5209.
[39] P.J. Bonasia, V. Christou, J. Arnold, J. Am. Chem. Soc. 115 (1993) 6777.
[40] C. Marschner, Eur. J. Inorg. Chem. (1998) 221.
[41] C. Kayser, G. Kickelbick, C. Marschner, Angew. Chem. 114 (2002) 1031.
[42] C. Kayser, R. Fischer, J. Baumgartner, C. Marschner, Organometallics 21 (2002) 1023.
[43] R. Fischer, D. Frank, W. Gaderbauer, C. Kayser, C. Mechtler, J. Baumgartner, C. Marschner, Organometallics 22 (2003) 3723.
[44] H. Lange, U. Herzog, J. Organomet. Chem. 660 (2002) 36.
[45] U. Herzog, G. Roewer, Main Group Met. Chem. 22 (1999) 579.
[46] U. Herzog, J. Prakt. Chem. 342 (2000) 27.
[47] U. Herzog, Main Group Met. Chem. 24 (2001) 31.
[48] H. Lange, U. Herzog, H. Borrmann, G. Roewer, in: N. Auner, J. Weis, Organosilicon Chemistry VI, Wiley–VCH, Weinheim (in print).
[49] M. Lardon, J. Am. Chem. Soc. 92 (1970) 5063.
[50] H.C.E. McFarlane, W. McFarlane, J. Chem. Soc., Dalton Trans. (1973) 2416.
[51] Bruker AXS Inc., Madison, WI, USA, 1998.
[52] Area-Detector Absorption Correction, Siemens Industrial Automation Inc., Madison, WI, USA, 1996.
[53] Crystal Clear, Rigaku Corp., 2000.
[54] A. Altomare, M.C. Burla, M. Camalli, G.L. Cascarano, C. Giacovazzo, A. Guagliardi, A.G.G. Moliterni, G. Polidori, R. Spagna, J. Appl. Cryst. 32 (1999) 115.
[55] G.M. Sheldrick, SHELX97 (includes SHELXS97, SHELXL97, CIFTAB), Programs for Crystal Structure Analysis, Release 97–2, University of Göttingen, Göttingen, Germany, 1997.
[56] M. Berndt, K. Brandenburg, H. Putz, DIAMOND 2.1: Crystal Impact GbR, Bonn, Germany, 1999. Available from: <www.crystalimpact.de>.
[57] H. Sakurai, K. Tominaga, T. Watanabe, M. Kumada, Tetrahedron Lett. (1966) 5493.
[58] R. Lehnert, M. Höppner, H. Kelling, Z. Anorg. Allg. Chem. 591 (1990) 209.
[59] U. Herzog, G. Rheinwald, Eur. J. Inorg. Chem. (2001) 3107.